International Journal of Automotive Technology, Vol. 7, No. 6, pp. 681−686 (2006)

1229−9138/2006/030−06

TECHNIQUE OF SEPARATE MEASURING SIDE SLIP FOR TOE ANGLE AND CAMBER ANGLE

H. NOZAKI*

Department of Mechanical Engineering, Faculty of Science and Engineering, Kinki University, 3-4-1 Kowakae, Higashiosaka-shi 577-8502, Japan

(Received 29 June 2005; Revised 18 July 2006)

ABSTRACT−The current flat type side slip tester measures only the total side slip. Therefore, measurement techniques which can be used to determine the side slip for each alignment element were examined. Because the side slip related to the camber angle varies depending on the unit load per travel wheel while the side slip related to the toe angle does not on the unit per travel wheel, but depends only on the direction of the tire, the side slip for each alignment element can be determined separately.

KEY WORDS : Wheel alignment, Test facility (test equipment), Side slip, Toe angle, Camber angle

1. INTRODUCTION

A flat type side slip tester was used to measure the total amount of side slip, which is a function of the toe angle, the camber angle, and the ply steer and conicity of the tire. It is possible, however, to have a situation where the influences of two elements, e.g., the toe angle and the camber angle, cancel each other, resulting in the total side slip being within the permissible range. This problem is being addressed at present in the market. A new scheme for measuring the side slip for individual alignment elements was examined and experiment devices were developed and investigated.

2. ALIGNMENT SEPARATION MECHANISM

The mechanism of alignment separation is discussed in the next section based on theoretical equations. The side slip related to the camber angle was found to vary according to the load per wheel (Sakai, 1987), and the side slip related to the toe angle was found to depend solely on the tire travel, and not on the load per wheel (Refer to the book by Sakai, 1987, 2000). Thus, it is possible to determine the total side slip. In addition, the side slip related to the ply-steer and conicity of the tire depends on the load per wheel, as shown by the rough sketch in Figure 1. Therefore, the side slip related to individual alignment elements can be determined easily.

**Corresponding author.* e-mail: nozaki@mech.kindai.ac.jp

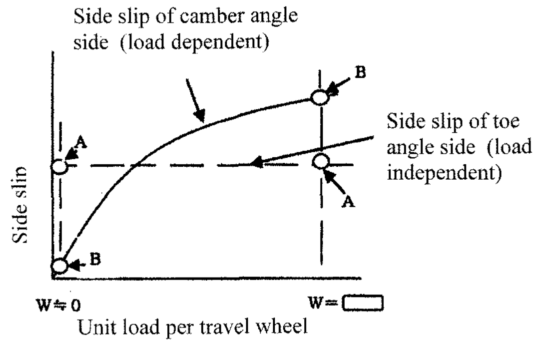

Figure 1. Change in side slip with unit load per travel wheel.

3. THEORETICAL EQUATION OF SIDE SLIP

3.1. Side Slip Related to Toe Angle

The present study examines a flat type side slip tester in which the transformation element due to the lateral power from the tires is 1 m in the lateral direction of the rolling of the tire. Details are provided in reference (Yamazaki *et al.*, 1993). In addition, the roller type sideslip tester was examined by Nishiyama (1999; Nishiyama *et al.*, 1999a, 1999b). The side slip in which the initial transformation element of the tire is liberated is described in the following.

The side slip due to the transformation by the lateral power of the tire is designated S_1, which is given below:

$$S_1=(K\cdot\gamma/L_F)\cdot\cos\gamma \tag{1}$$

K: cornering power
γ: toe angle
L_F: tire lateral rigidity

Note that this element is liberated in the roller type side slip tester when the tire boards the roller. Therefore, in the case of the roller type side slip tester, we have S_1=0.

Next, the side slip in the lateral direction when tire rolls 1 m is described.

The side slip in the lateral direction of the rolling of the tire by 1 m is designated S_2, which is given below:

$$S_2=2\pi R \cdot n \cdot \tan\gamma \tag{2}$$

R: radius of roller
n: number of rotations ($2\pi R{\cdot}n=1m$)
γ: toe angle

In the roller side slip tester, the only element detected in equation (2) is the toe angle element, which is a geometrical element.

3.2. Side Slip Related to Camber Angle

The part where the tire touches the ground is transformed by generating lateral power between the tire and the road when the camber angle is given to the tire. The side slip is herein obtained as the sum of the amount by which the transformation element of the tire is liberated and the side slip in the lateral direction when the tire has rolled for 1 m.

The amount by which the transformation element of the tire is liberated at a camber angle of ϕ is given below.

The transformation by the lateral power of the tire is designated S_3, which is given below:

$$S_3=K_t \cdot \phi/L_F \tag{3}$$

K_t: camber stiffness
ϕ: camber angle
L_F: tire lateral rigidity

Note that this element is liberated in the roller side slip tester when the tire boards the roller. Therefore, in the case of the roller side slip tester, we have S_3=0.

The side slip in the lateral direction when a tire with camber rolls 1 m is described as follows.

When the camber angle is given as shown in Figure 2, the ground length of the tread base l_r from the ground start point A is approximately equal to the arc ACB. However, because the tread base has side bend rigidity, the circular arc $AC'B$, which is a better approximation than ACB, is tracked, and tread rubber passes in a straight line along segment AB. This camber thrust is thought to cause shear between the tread base, which scans a circular arc, and the tread rubber, which moves in a straight line.

The tread base is thought to scan the circular arc $AC'B$ of radius r', as shown in Figure 3. The camber thrust C_r is given by the following equation if the area of circular arc $AC'BD$ is assumed to be A_1:

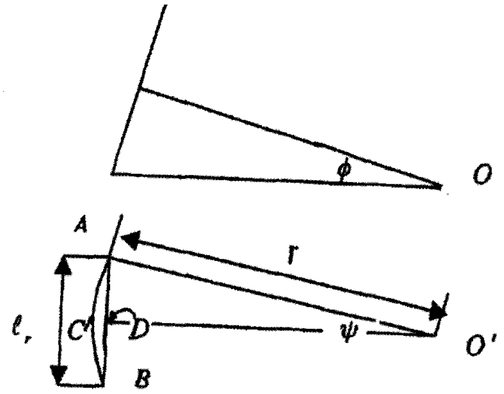

Figure 2. Intuitive pass of tread base (having camber angle).

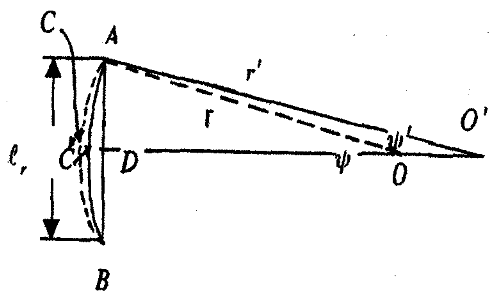

Figure 3. True pass of tread base (having camber angle).

$$C_r=A_1C_x \cdot b_r=K_t\phi \tag{4}$$

C_x: rigidity of shear for each unit length of tread rubber
b_r: effective tread width
K_t: camber rigidity
ϕ: camber angle

Area A_2 of sector $O'AB$ is given as follows:

$$A_2=\frac{l_r \cdot r'}{2} \tag{5}$$

where: $\left[A_2=\psi' r'^2,\ \psi'=\frac{l_r}{2r'}\right]$

Area A_3 of triangle $O'AB$ is given as follows:

$$A_3=\frac{l_r r'}{2}\left(1-\frac{l_r^2}{8r'^2}\right) \tag{6}$$

Therefore, area A_1 is given as follows:

$$A_1=A_2-A_3=\frac{l_r^3}{16r'} \tag{7}$$

The curve rate radius when the ground transformation of the tread base is given by equations (4) and (7).

$$r'=\frac{l_r^3 b_r C_x}{16K_t\phi} \tag{8}$$

where: $\left[\frac{l_r^3}{16r'}C_x b_r=K_t\phi\right]$

The roller moves in the tangent direction at point A of radius r' when point A of the ground start of the tire is approximately equal to the track along a circle of radius r' of the tire rolling. Therefore, the side slip S_4 is given as follows:

$$S_4=2\pi R\cdot n\cdot\tan\psi' \tag{9}$$

R: roller diameter
n: number of rotations

Moreover, the relationship between ψ' and r' is as follows:

$$r'\sin\psi'=l_r/2 \tag{10}$$

where:

$$\left[\sin\psi'=\frac{l_r}{2r'}=\frac{l_r}{2}\cdot\frac{16K_t\phi}{l_r^3 b_r C_x}=\frac{8K_t\phi}{l_r^2 b_r C_x}\right]$$

If equation (9) is obtained from equations (8) and (10), then equation (9) can be rewritten as follows:

$$S_4=K_t\phi\cdot\left(2\pi R\cdot n\cdot\frac{8}{l_r^2 b_r C_x}\right) \tag{11}$$

If the curve rate radius r' when the tread base is grounded is needed, equation (9) shows that the side slip S_4 can be obtained by the geometrical method, as shown in Figure

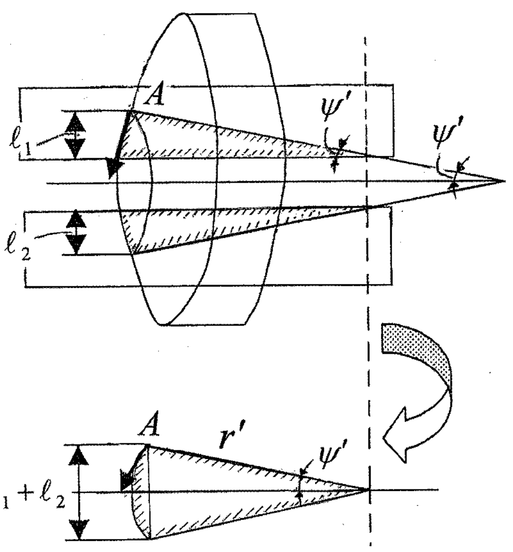

Figure 4. Intuitive pass of the tread base (having camber) for the roller tester of the present study.

3. Next, the method for approximating S_4 is considered (refer to Figure 5 in Section 4), as shown in Figure 4.

Therefore, the roller moves in the direction of the tangent of point A of radius r' when point A of the ground start point of the tire is about to scan a circle of the radius r' (to the approximation target). Therefore, the side slip S_4 can be given by equation (9) in the same manner as mentioned above.

Moreover, the relationship between ψ' and r' given in the following equation is obtained:

$$r'\sin\psi'=(l_1+l_2)/2 \tag{12}$$

Therefore, the following equation is thought to be a rugged structure as mentioned above and is derived from equation (11).

$$S_4=K_t\phi\cdot\left(2\pi R\cdot n\cdot\frac{8}{(l_1+l_2)^2 b_r C_x}\right) \tag{13}$$

That is, equation (13) is approximately equivalent to equation (11) through the following replacement: $l_r \Rightarrow (l_1+l_2)$.

4. EXPERIMENTAL DEVICE

An experiment was conducted to measure the side slip using two rollers, as shown in Figure 5, so that the side slip related to individual alignment elements can be determined. The side slip related to the toe angle was determined using a smaller roller that barely contacted the tire. The larger roller was used to measure the total side slip, and the smaller roller was used to measure the toe angle side slip only. The camber angle side slip could then be calculated by subtracting the toe angle side slip from the total side slip (Figure 5). The experimental device was then constructed and investigated. The slider mechanism in the lateral direction to the roller was assumed to have the form shown in Figure 6. In the

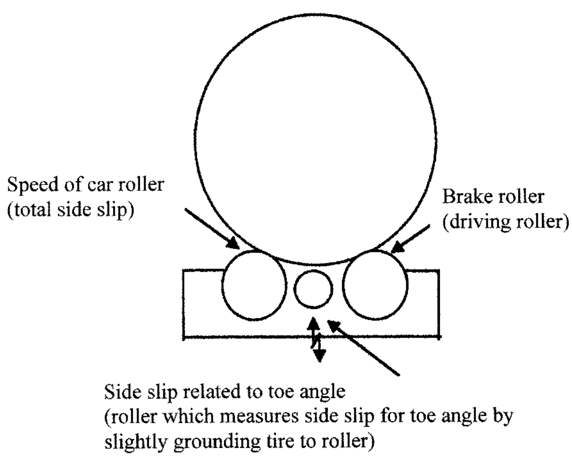

Figure 5. Schematic diagram of the experimental device.

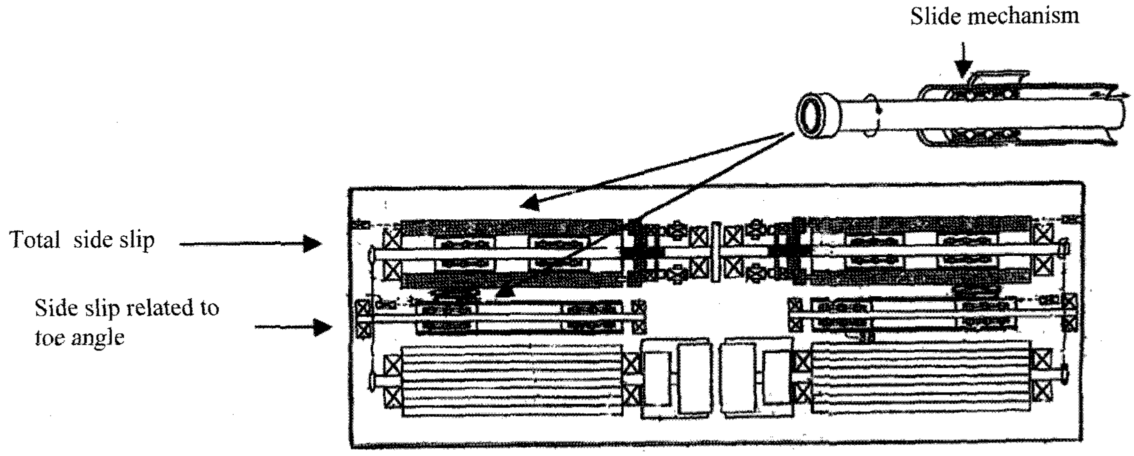

Figure 6. Roller tester of the present study (slide mechanism).

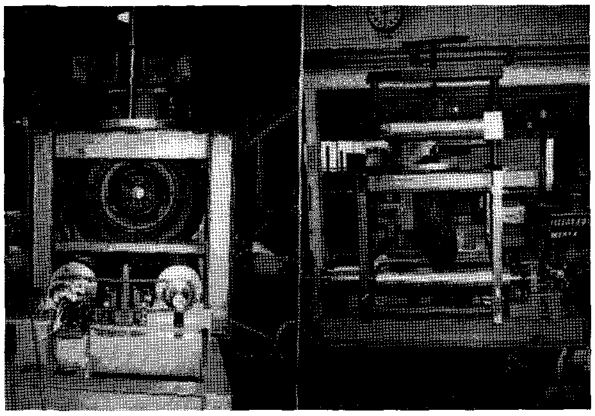

Figure 7. The variable-alignment tire suspension system.

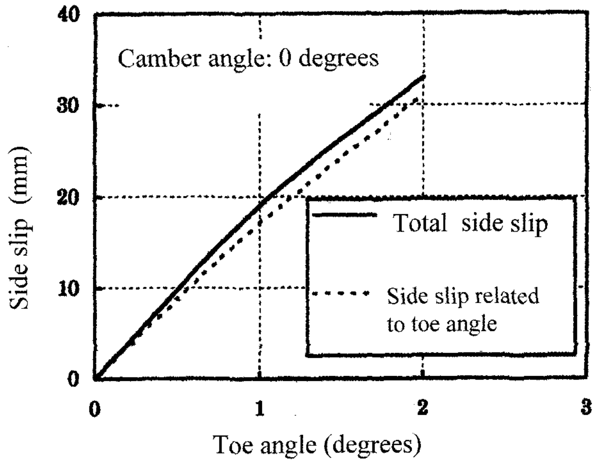

Figure 8. Effect of toe angle on side slip (6.40 R14 Tire).

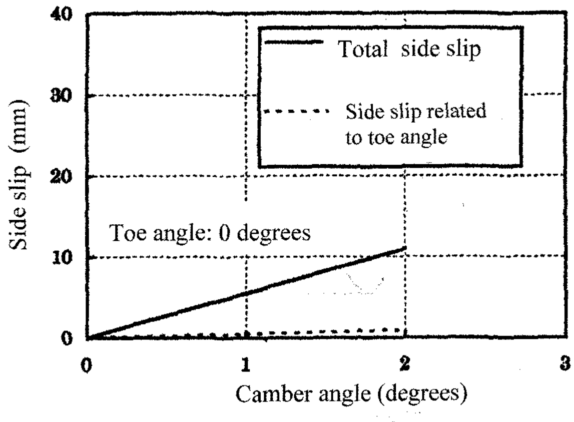

Figure 9. Effect of camber angle on side slip (ex. 6.40 R14 Tire).

experiment, in order to individually vary parameters such as the toe angle, the camber angle, and the unit load per travel wheel, a variable-alignment tire suspension system was constructed, and a bench test was performed (Figure 7). In addition, a confirmation experiment was performed by examining a real car.

5. EXPERIMENTAL RESULTS AND CONSIDERATION

5.1. Experimental Results

The experimental results obtained on the test stand with the variable alignment tire support device are described in this section. The side slip was found to be similar for both detection rollers when only the toe angle was changed (camber angle: 0 degrees) (Figure 8).

On the other hand, the larger detection roller (roller for total side slip detection) registered increased side slip when only the camber angle was changed (toe angle: 0 degrees). It was confirmed that little side slip occurred at the smaller detection roller (roller for the detection of side slip related to toe angle) because the unit load per travel wheel of the side slip detection roller for the toe

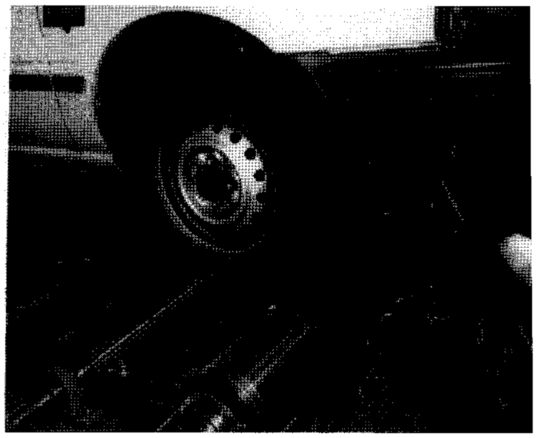

Figure 10. Placement of the roller tester in the present study.

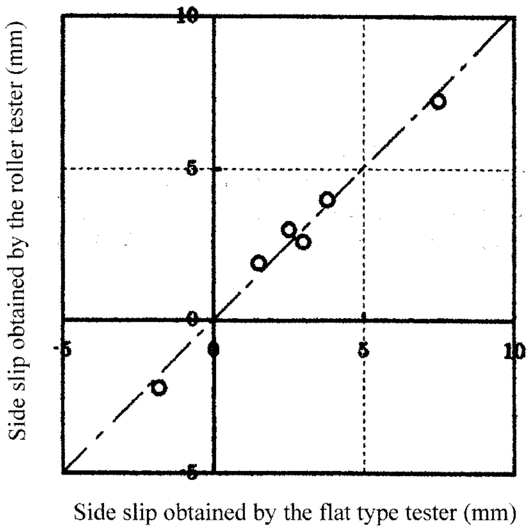

Figure 11. Side slip as obtained by the flat type tester and the roller tester in the present study.

angle was approximately zero (Figure 9). Therefore, it was clarified that detection of the side slip related to individual alignment elements is possible using these two side slip detection rollers.

The experimental results obtained for an actual car are described below. Figure 10 shows a photograph of the experiment. Figure 11 shows the experimental results for six vehicles. The experimental results for the side slip are compared with the measurement results obtained using the flat type side slip tester and those obtained using the roller side slip tester. No large difference was observed between the obtained values. Therefore, the roller tester can be used to determine the side slip of an actual car. Moreover, in this section the problem of the toe angle is shown by a flow chart, while in the next section for the

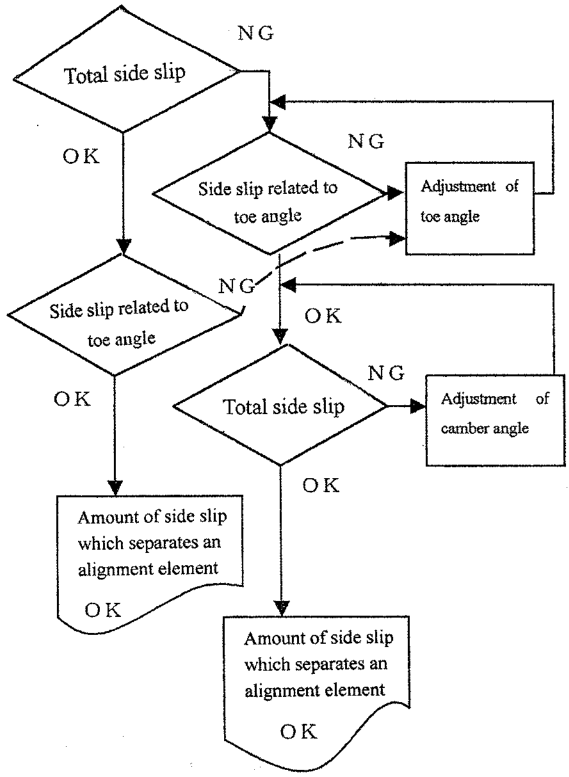

Figure 12. Flow chart for side slip judgment related to individual elements.

case when the side slip exceeds 5 mm is considered.

5.2. Technique for Judging Quality

Basically, when a quality judgment is made, as in the following flow chart, it is possible to make a quality judgment of the side slip based on individual alignment elements. In Figure 12, the relational equation is as follows.

$$(\text{side slip related to toe angle}) = 1000 \times \tan(\text{toe angle}) \quad (14)$$

The quality can be judged by converting the alignment control value for the toe angle into the side slip related to the toe angle.

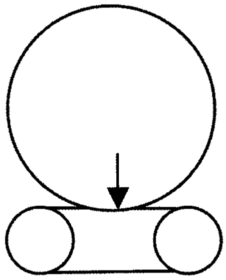

Figure 13. Flat belt type side slip tester.

5.3. Considerations for Improving Measurement Accuracy

The measurement of the side slip related to individual alignment elements is possible using a roller side slip tester. However, because of differences between the actual road/tire interface and the roller shape, the curve rate of the roller has a minute influence on the measurement of the side slip. Therefore, it is preferable to match the actual road/tire interface as closely as possible, for example by using a flat belt type structure, such as that shown in Figure 13 and to improve the measurement accuracy in the future.

6. CONCLUSIONS

A new scheme that can measure the side slip related to individual alignment elements was considered, and the following conclusions were obtained:

(1) The side slip related to the camber angle was found to vary according to the load per wheel, and the side slip for the toe angle was found to depend solely on the tire travel and not on the load per wheel. Therefore, it is possible to determine the total side slip.

(2) When the measurement described in (1) becomes possible, quality judgment related to various alignments becomes possible using the equation for the side slips related to the toe angle and camber angle. Therefore, although a situation in which two negative alignments is possible, for example, negative toe angle and negative camber angle, these alignments cancel each other, resulting in the total side slip being within the permissible range. Moreover, this problem can be improved using the roller side slip tester examined in the present study.

Although the side slip tester is an effective device for determining the overall influence of the alignment elements of a vehicle, the proposed scheme can be used to measure the side slip due to individual alignment elements. The effect of the roller curvature will be examined in future studies.

REFERENCES

Yamazaki, S., Fujikawa, T. and Yamaguchi, I. (1993). An analytical study on measurement principle of a side slip tester. *J. Society of Automotive Engineers of Japan (JSAE)*, **24-4**, 70–75. (in Japanese).

Nishiyama, S., Harada, S., and Harada, K. (1999a). Development of a roller-type side slip tester. *J. Society of Automotive Engineers of Japan (JSAE)* **30-1**, 109–114. (in Japanese).

Nishiyama, S. (1999). Research on roller-type side slip tester (theoretical and experimental investigation on measurement principles). *Trans. Japan Society of Mechanical Engineers* (*JSME*), **65-630**, **C**, 564–571. (in Japanese).

Nishiyama, S., Harada, S., and Harada, K. (1999b). Development of a roller-type side slip tester (performance test with real automobiles), *Trans. Japan Society of Mechanical Engineers* (*JSME*), **65-633**, **C**, 1973–1977. (in Japanese).

Sakai, H. (1987). *Tire Engineering*. Grand Prix Publication, 168, 404–407. (in Japanese).

Sakai, H. (2000). *Secret of Tire Which Supports Running*. Mokabou Publication. (in Japanese).